Conduction in Charged PbSe Nanocrystal Films

Brian L. Wehrenberg, Dong Yu, Jiasen Ma, and Philippe Guyot-Sionnest*

James Franck Institute, University of Chicago, Chicago, Illinois 60637

Received: July 1, 2005; In Final Form: August 12, 2005

Conduction in thin films of PbSe nanocrystals doped by electrochemical gating has been studied. Charging the film, with either electrons or holes, increases the conductance by orders of magnitude. The electrons in the $1S_e$ state of nanocrystals in these films have a mobility as high as 5.0×10^{-3} cm^2 V^{-1} s^{-1}. Electrons in the $1P_e$ state were found to have a differential mobility up to 3−5 times greater than the electrons in the $1S_e$ state, and a mobility minima was found corresponding to the complete filling of the $1S_e$ state. The temperature and electric field dependence of conductance in the film, measured between 4.3 and 135 K, were both well described by a variable range hopping model.

I. Introduction

Since the publication of the initial report on the synthesis of highly monodisperse PbSe colloidal nanocrystals, there has been an explosion of interest in the field.[1] Much of the interest in these nanocrystals is due to their strong interband transitions in the IR, which can easily be tuned with size, from 0.5 to 1 eV.[2,3] IR electroluminescence,[4] amplified stimulated emission,[5] and high quantum yield photoluminescence[2,6] have all been reported for this system. Recently, high-efficiency multiple exciton generation has been discovered in PbSe nanocrystals, making PbSe nanocrystals a promising system for incorporation into solar cells and photodetectors.[7−9] The ability to successfully and efficiently incorporate PbSe nanocrystal architectures into optoelectronic devices requires a fundamental understanding of the effects of charge and the conduction of charge in this system. With this in mind, we have studied the conduction properties of charged thin films of PbSe colloidal nanocrystals.

The conduction properties of arrays of semiconductor nanocrystals have been studied previously. Arrays of uncharged CdSe nanocrystals were found to be insulating for fields up to 10^6 V/cm.[10] However, upon electron injection into the quantum-confined states of the nanocrystals by electrochemical gating, the conductivity of the films was seen to increase by several orders of magnitude.[11] At low temperature, the conduction in these CdSe thin films was accurately described by a variable range hopping model.[12]

Building upon our previous work on electron and hole injection into thin films of PbSe nanocrystals,[13] we extend our study to the quantitative injection of electrons into the $1S_e$ state via electrochemical gating. We then utilize this quantitative electrochemical charge injection to measure the mobilities of electrons and holes in the film. Finally, the low-temperature behavior of the conductance and its field and temperature dependence are explored.

II. Experimental Section

The PbSe colloidal nanocrystals in this paper are prepared as reported in the literature.[2] This synthesis results in highly monodisperse nanocrystals capped in oleic acid. After synthesis, the nanocrystals are precipitated from the reaction mixture with acetone. The nanocrystals are then "cleaned" by dissolving them in a small amount of chloroform, precipitating the dots with methanol, centrifuging the solution, decanting the supernate, and rinsing the precipitate with methanol. This procedure removes excess organic capping molecules from the nanocrystal solution. For film preparation, the PbSe nanocrystals are dissolved in a 9:1 hexane/octane mixture.

For the spectroelectrochemical measurements, the working electrode is a slide of indium tin oxide (ITO)-coated float glass 0.7 mm thick from Delta Technologies. The ITO electrode was placed into a 50 mM solution of 3-mercaptopropyltrimethoxysilane in acetone for over an hour to functionalize the ITO for bonding with the dots. After the electrodes are rinsed with chloroform, they are then baked at 120 °C for 30 min. After they are baked, the electrodes are allowed to cool in a vacuum before being brought into the glovebox for film deposition. Film preparation and assembly of the electrochemical cell are performed under a nitrogen atmosphere to minimize exposure to oxygen and water. A drop of the nanocrystals in the hexane/octane solution is deposited on the ITO. As soon as the film appears dry, it is dipped into a 5 mM solution of 1,7-diaminoheptane in methanol for over 1 min. The film is then heated to 70 °C in a nitrogen atmosphere for an hour and placed under vacuum for several hours. This treatment makes the film more mechanically stable and also speeds the charging, and discharging, of the film.[13,14]

The spectroelectrochemical cell is a modified absorption cell with a 0.2 cm path length. To further minimize exposure to oxygen and water, the cell is airtight. The ITO electrode with the nanocrystal thin film is held suspended in the absorption cell along with a platinum counter electrode and a silver pseudoreference electrode. All electrochemical potentials reported herein are relative to this Ag pseudoreference. The cell is then filled with 0.1 M $LiBF_4$ in acetonitrile. For spectroelectrochemical measurements, the cell is transferred to an FTIR, which was continuously purged with nitrogen.

For all other electrochemical measurements and for the low-temperature conduction measurements, the films are prepared on interdigitated microsensor electrodes (IMEs) from Abtech Scientific. The IMEs consist of 50 pairs of 15 μm wide platinum digits separated from each other by 15 μm on a glass chip. Each

* To whom correspondence should be addressed. E-mail: pgs@uchicago.edu.

10.1021/jp053621t CCC: $30.25
Published on Web 09/29/2005

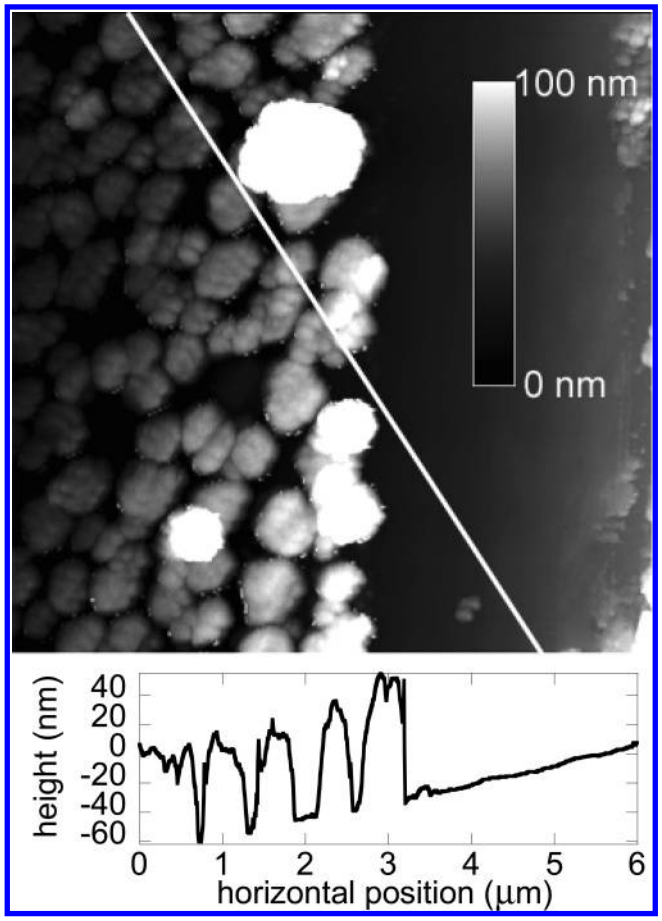

Figure 1. Topographical image of a film of PbSe nanocrystals on a silane-treated glass substrate taken by AFM in tapping mode. The dark region on the right is part of a trench cut into the film by a razor blade. The area imaged is 5 μm by 5 μm. The diagonal white line is the location of the cross-section shown below the image.

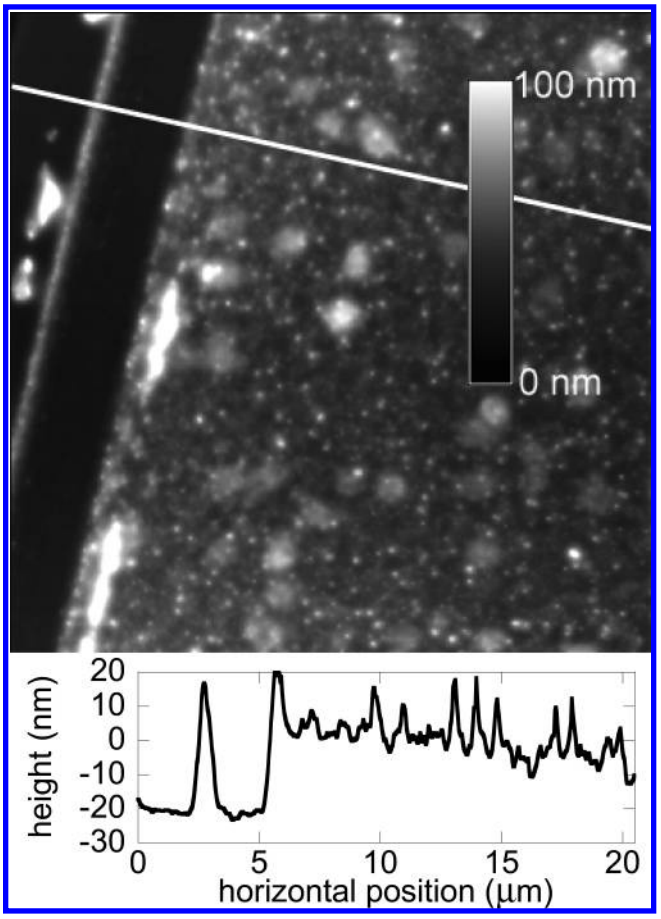

Figure 2. Topographical image of a film of PbSe nanocrystals taken by AFM in tapping mode. The nanocrystals in the film are from the same sample used to make the film in Figure 1, but they have been washed with ethanol three times. The area imaged is 20 μm by 20 μm. The dark area on the left is the edge of a cut made in the film by a razor blade. Below the image is the cross-section of the film taken from the location of the white line in the image.

platinum digit is 5 mm in length with a 110 nm thickness. Prior to drop casting, the electrodes are treated by dipping them into a solution of 10 mM 1,6-hexanedithiol in chloroform for at least 1 h. After the electrodes are rinsed with chloroform, they are heated in a 70 °C oven for 30 min. This treatment effectively functionalizes the electrode surface for bonding with the nanocrystals. After the IMEs are allowed to cool in a vacuum, they are then brought into the glovebox for deposition of the nanocrystal film. After deposition, the film is treated with 1,7-diaminoheptane in a manner identical to the films on ITO.

Initially, films made in this manner on IMEs were found to have conduction properties which were not reproducible, bringing the quality of the films into question. To explore film quality, films of PbSe nanocrystals are drop cast onto a glass substrate which has been pretreated with 3-mercaptopropyltrimethoxysilane. The film is then treated with 1,7-diaminoheptane as described above. A razor blade is gently drawn across the film to cut through the film but not cut into the glass. This allows us to get information about the height of the film on the glass. The film was then imaged near the cut with an atomic force microscope (AFM) in tapping mode.

Figure 1 shows a film made with PbSe nanocrystals after only their original cleaning with methanol. One can clearly see that the film is not continuous across the glass substrate. Instead, the nanocrystals form monolithic plateau structures on the glass substrate. It appears that between these structures there are areas of the glass with no nanocrystals on the substrate. This is clearly not a good film for conduction studies.

We hypothesized that perhaps an excess of capping molecules causes the nanocrystals to form these monolithic structures, and thus, we endeavored to clean the nanocrystal solution more thoroughly. However, simply cleaning the nanocrystal solution again with methanol removes too many of the capping molecules, and the nanocrystals either are no longer soluble or tended to aggregate during the drying of the film, causing a grainy film. Apparently, there is a delicate balance between having excess and not having enough capping molecules for proper film preparation. Cleaning with ethanol proved to be a gentler way to remove the caps. Figure 2 shows another film of PbSe on a glass slide treated with 3-mercaptopropyltrimethoxysilane. After an initial methanol wash, three ethanol washes were performed on the sample of nanocrystals which was used to make this film. The resulting film appears to be continuous across the treated glass substrate and shows a marked increase in quality over the film in Figure 1. The exact number of ethanol washes needed to make good quality films varies from sample to sample but is usually between two and four. It should be noted that AFM images of films made from CdSe nanocrystals capped with trioctylphosphine oxide do not exhibit this delicate balance and almost always form continuous films.

The IMEs are installed into a Teflon electrochemical cell for electrochemical and conduction measurements. The cell is an airtight Teflon container with a silver pseudoreference electrode, a platinum counter electrode, and Pt−Ir clips to connect to the

IMEs. Once again, a solution of 0.1 M $LiBF_4$ in acetonitrile acts as the electrolyte.

The Teflon cell is placed in a liquid helium Dewar. The temperature of the electrochemical cell can be changed by varying the height of the cell above the liquid helium. Electrochemical measurements are taken in the −40 to −50 °C range to clean up the electrochemistry of the films by removing, or reducing, currents that compete with the charging of the nanocrystals in the thin films. Electrochemical measurements involving films prepared on the IMEs are made with a bipotentiostat. The bipotentiostat allows the potential of two interdigitated electrodes to be varied with respect to each other and with respect to the silver pseudoreference. The interdigitated platinum working electrodes can thus be scanned while holding a static bias (usually ∼5 mV) between the two electrodes. During a scan, the sum of the two working electrode currents is the total electrochemical current and one-half of the difference between the two currents is the conduction current.

For the low-temperature conduction measurements, the films are quickly cooled below the freezing point of the electrolyte by immersing the cell into liquid helium while the potentials of the working electrodes are held in a region where the film is charged. This step immobilizes the counterions in the electrolyte, trapping charges in the nanocrystal thin film. Just before the electrolyte freezes, the electrodes must be disconnected from the bipotentiostat. If the electrodes are not disconnected, the reference electrode would become electrically disconnected from the working electrodes upon freezing. Then, the bipotentiostat would apply large and uncontrolled voltages to the counter electrode which could either discharge the film or even cause damage to the sample. This early disconnection, coupled with a temperature-dependent shift in the electrochemical charging potentials of the dots, leads to an uncertainty in the exact charging level of the quantum dots. The temperature of the film is easily varied by simply changing the depth of the cell in the liquid helium. In this way, IV curves can be collected in the range from 4.3 to 135 K. At these low temperatures, the system is remarkably stable. The IV curves collected days apart but at the same temperature were always identical and independent of the temperature history as long as the samples remained in the temperature region listed above. Once above 135 K, the films slowly discharge.

III. Results and Discussion

A. Quantitative Spectroelectrochemistry. Previously, we reported on the electrochromic response of thin films of PbSe colloidal nanocrystals upon injection of charge into the quantum-confined states of these nanocrystals.[13] We found that with the application of an increasingly negative potential, the $1S_e$ and $1P_e$ states of the quantum dots could be sequentially filled. The injection of charge into the $1S_e$ state was confirmed by a bleach of the first exciton accompanied by an induced intraband absorption. However, at that time, it was impossible to quantitatively determine the number of electrons needed to fill the $1S_e$ state. Spectroelectrochemical measurements on thin films of CdSe quantum dots were able to determine that an average of two electrons per dot could be injected into the $1S_e$ state.[14] In the bulk, PbSe is known to have fourfold degenerate valence and conduction band extrema at the L points of the Brillouin zone.[15] This means that the $1S_e$ state should hold eight electrons. In this section, quantitative low-temperature spectroelectrochemistry of a thin film of PbSe colloidal nanocrystals is used to determine the degeneracy of the $1S_e$ state in PbSe nanocrystals.

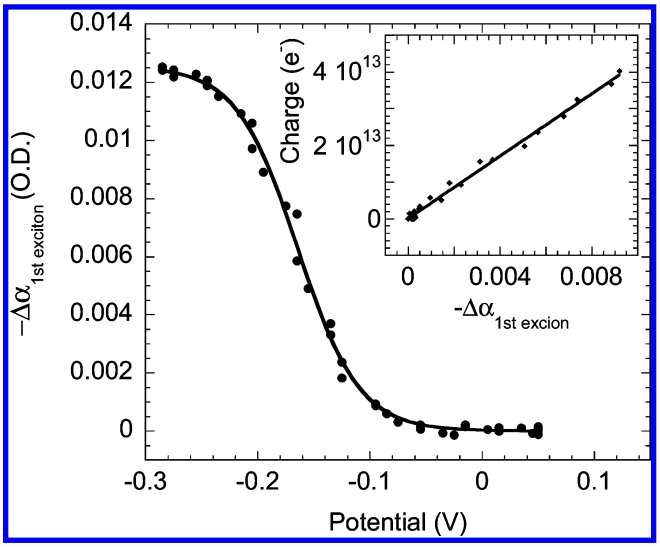

Figure 3. Bleach of the first exciton optical density as a function of the potential applied to the film of PbSe nanocrystals. The nanocrystals have a first exciton at 0.60 eV. The solid line is a guide to the eye, as described in the text. Inset: the integrated charge in the film determined from electrochemistry plotted against the corresponding first exciton bleach.

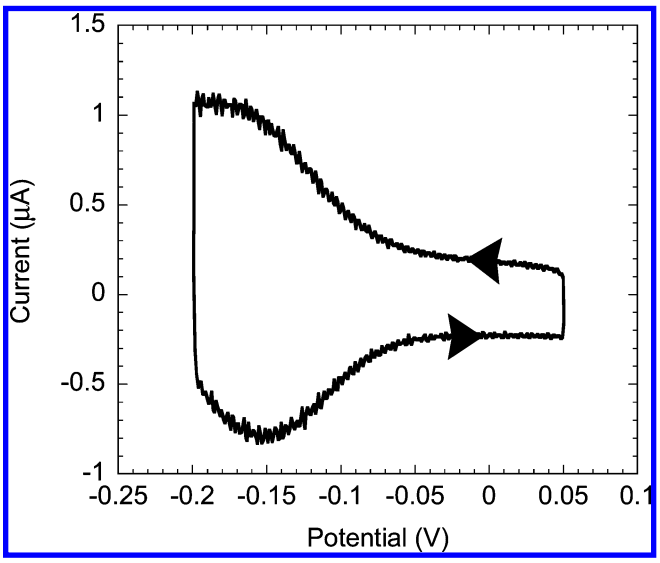

Figure 4. Cyclic voltammetry of a film of PbSe nanocrystals with first exciton at 0.60 eV. Voltammetry was performed at −35 °C with a 10 mV/s scan rate. Arrows show the direction of scan.

In this experiment, cyclic voltammetry of a film of PbSe nanocrystals with a first exciton at 0.6 eV was performed at −35 °C with a scan rate of 10 mV/s. IR spectra were taken every 4 s during the cycle to track the bleach of the first exciton. Shown in Figure 3 is the magnitude of the first exciton bleach plotted vs the potential applied to the film. From the IR spectra it can be determined that the −0.3 V potential applied here is enough to completely charge the $1S_e$ state and partially charge the $1P_e$ state. In Figure 3, a one-electron thermal equilibrium fit is used as a guide to the eye, in which the magnitude of the bleach is proportional to $1/(\exp(e(V - V_R)/k_BT) + 1)$, where V is the potential, V_R is the reduction potential of the nanocrystal, k_B is Boltzmann's constant, and T is an adjustable "temperature".

Figure 4 shows the cyclic voltammetry of the same sample. In the potential range used in this cycle, electrons only charge the $1S_e$ state. The total amount of charge flowing to and from the working electrodes can be determined by integrating one full cycle of the cyclic voltammetry. The capacitance of the

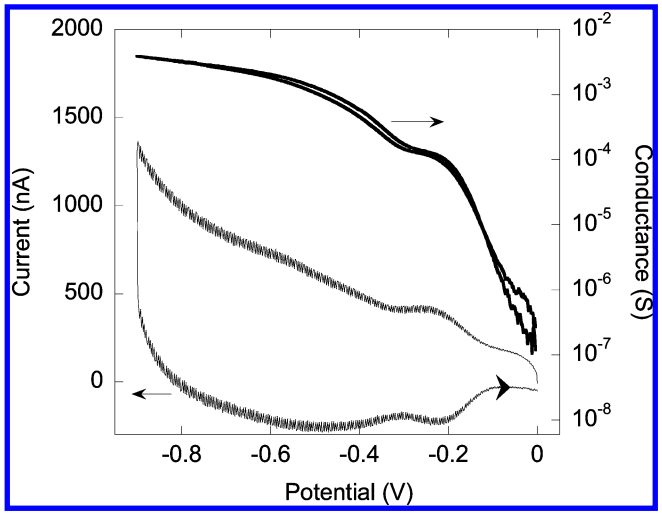

Figure 5. Cyclic voltammetry and conductance of a film of PbSe nanocrystals on IMEs taken at −48 °C with a scan rate of 10 mV/s and 5.2 mV bias applied between the working electrodes. The nanocrystals have a room-temperature first exciton at 0.66 eV. The arrow on the voltammetry curve shows the direction of the scan.

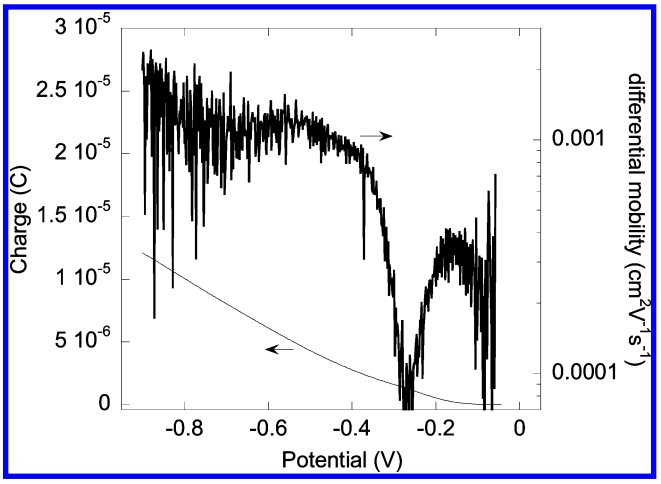

Figure 6. Integrated charge and the differential mobility of a film of PbSe nanocrystals on IMEs taken at −48 °C with a scan rate of 10 mV/s and 5.2 mV bias applied between the working electrodes. The data are from the cyclic voltammetry shown in Figure 5.

electrode is then subtracted to yield the total amount of charge that flows into and then back out of the film of nanocrystals. The integrated charge in the film at any given point of the cycle is then simply one-half of this quantity. If this integrated charge is plotted vs the magnitude of the first exciton bleach, then a linear relationship is determined, as shown in the inset to Figure 3. From the slope of this line and the area of the film, the per electron optical cross-section at the first exciton peak is calculated to be 4.2×10^{-16} (±15%) cm^2.

Since the optical cross-section of a PbSe colloidal nanocrystal has yet to be reported, we have undertaken a simple experiment to determine this value and thus the number of electrons that can be injected into the $1S_e$ state. A known amount of tetrachloroethane is added to an unknown amount of PbSe nanocrystals with a 0.6 eV first exciton. After a spectrum of the solution is recorded, to determine its optical density at the first exciton, the solvent is dried and the amount of lead in the sample is determined by inductively coupled plasma. Since the diameter of the nanocrystals is known from TEM measurements to be 8.1 nm, the number of nanocrystals and thus the optical cross-section of a single PbSe nanocrystal can be calculated. The value for the optical cross-section of a PbSe nanocrystal is 2.5×10^{-15} (±15%) cm^2 at the first exciton peak. Having determined an estimate for the cross-section of a PbSe nanocrystal, simple division gives us that 5.9 (±20%) e^- can be injected into the $1S_e$ state of a PbSe nanocrystal. This estimate is in fair agreement with the eight electrons per dot from both theory and previous optical experiments[5,15] and demonstrates the ability to quantitatively account for charges injected into a film. In the next section, this ability will help us to determine the mobility of charges in the thin films of charged PbSe nanocrystals.

B. Electrochemical Charging and Conduction. Previously, it was found that the conductance of films of CdSe and ZnO nanocrystals showed a marked increase upon injection of electrons by electrochemical gating.[11,16] In this section, we explore the effect that charging has on conductance in thin films of PbSe nanocrystals. Figure 5 shows the cyclic voltammetry of a film of PbSe quantum dots with a first exciton at 0.66 eV deposited on the IMEs. The electrochemical cell was kept at a temperature of −48 °C during the cycle, and a 5.2 mV bias was maintained between the two working electrodes as the potential was swept at a 10 mV/s rate. Although it was not possible to take the spectroscopic measurements of the sample on the IMEs in situ, the cathodic peak shown at −0.25 V can be attributed, from prior spectroelectrochemical measurements, to the charging of the $1S_e$ state. Notice that there is also an anodic peak at almost the same potential corresponding to the discharging of the $1S_e$ state when the potential was returned to zero. The broader cathodic and anodic peaks at more negative potentials are then attributed, respectively, to the charging and discharging of the $1P_e$ state.

Also shown in Figure 5 is the conductance of the film determined from the current that flowed across the 15 μm gap of the IMEs during charging. Upon the injection of electrons into the $1S_e$ state of the nanocrystals, the conductance increases dramatically and then levels out near the potential where the $1S_e$ cathodic peak is located. After this plateau, the conductance of the film increases once again as electrons are injected into the $1P_e$ state. To better elucidate what is occurring during the charging process, Figure 6 plots the amount of charge that has been injected into the film as well as the differential mobility of the electrons. The amount of charge in the film, determined by integration of the area of the cathodic scan after subtracting the capacitance of the working electrodes, increases smoothly as the potential is swept more negative. However, the differential mobility of the electrons has a dip located between the $1S_e$ and $1P_e$ charging peaks. This phenomenon has previously been observed in films of CdSe nanocrystals.[11] For films of ZnO nanocrystals, a plateau, not a dip, was seen between the $1S_e$ and $1P_e$ charging peaks.[16]

The dip in the mobility of the electrons corresponds to having a completely filled $1S_e$ state in the nanocrystals. Because the $1S_e$ and $1P_e$ electronic states are energetically well separated, electrons cannot access the $1P_e$ state from the $1S_e$ state with the thermal energy available. Therefore, as the $1S_e$ state nears being full, one expects the mobility to drop as unoccupied $1S_e$ states in the film become more and more rare. Electron transfer from an occupied to unoccupied state should scale as $\chi(1 - \chi)$, where χ is the average filling fraction, meaning that a peak in the conductance should be observed at half filling of the state. Instead of a peak, a shoulder at half filling of the $1S_e$ state is observed in the data shown in Figure 5. This broadening of the peak into a shoulder is most likely due to the size dispersion of the sample of nanocrystals from which the film was made.

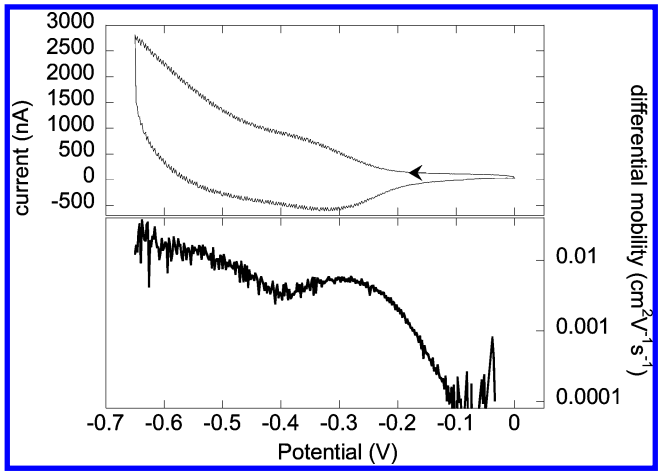

Figure 7. Cyclic voltammetry taken at −48 °C with a scan rate of 10 mV/s and 4.4 mV bias applied between the working electrodes. The arrow on the voltammetry curve indicates the scan direction. The PbSe nanocrystals in the film had a 0.7 eV room-temperature first exciton. The lower panel shows the corresponding differential mobility for the cathodic scan.

Figure 6 shows that $1P_e$ electrons have a higher differential mobility than that of the $1S_e$ electrons. The peak in the differential mobility of the $1S_e$ electrons, corresponding to a film of quantum dots with half-filled $1S_e$ states, is 3.5×10^{-4} $cm^2\ V^{-1}\ s^{-1}$. Whereas, the peak mobility of the $1P_e$ electrons was determined to be 1.2×10^{-3} $cm^2\ V^{-1}\ s^{-1}$. This ratio of the $1S_e$ electron mobility and $1P_e$ electron mobility varied slightly from film to film but was usually in the range of 3−5.

$1S_e$ electron mobilities up to an order of magnitude larger are observed in some films of PbSe nanocrystals. Figure 7 shows the electrochemistry and differential mobility for a film of PbSe nanocrystals with a room-temperature first exciton at 0.70 eV. The conductance of this film at −0.65 V is quite large, and thus, the resistance of the IMEs themselves is, in fact, larger than the resistance of the film. The conductance data is corrected for this by subtracting the resistance of the electrodes, which was measured to be 71 Ω, from the total measured resistance. While this correction has a large effect on the $1P_e$ differential mobility, the effect on the $1S_e$ differential mobility is small and thus the observed peak value for the $1S_e$ differential mobility of 0.5×10^{-2} $cm^2\ V^{-1}\ s^{-1}$ can be trusted. This corresponds to a conductivity on the order of 2×10^{-2} S cm^{-1}. The dip in mobility is also less pronounced in this film. This behavior is observed as well for the more conductive films of CdSe nanocrystals[11] but not understood.

The values for the $1S_e$ mobility reported here are several orders of magnitude larger than that observed in the thin films of CdSe colloidal nanocrystals cross-linked with 1,7-diaminoheptane.[11] Films of CdSe nanocrystals cross-linked with 1,4-phenylenediamine were found to have an $1S_e$ mobility 3 orders of magnitude larger than that of the CdSe films cross-linked with 1,7-diaminoheptane. Therefore, optimization of the cross-linker for films of PbSe colloidal nanocrystals holds promise for increasing the mobility even further.

Finding an optimal cross-linker should also help another aspect of the conductance in these films of PbSe. One of the most exciting features of PbSe nanocrystal thin films is the ability to dope them with both holes and electrons. However, as stated in a previous report, charging the film with holes is more difficult than with electrons. Total filling of the $1S_h$ state and even partial filling of the $1P_h$ state have not been spectroscopically observed with the current 1,7-diaminoheptane linkers.[13] In addition, the films become unstable when too high a positive electrochemical potential is applied. Despite these problems, we have seen conductance in films of PbSe nanocrystals cross-linked with 1,7-diaminoheptane charged with holes. Figure 8 shows the integrated positive charge injected into the film and the differential mobility for the holes in the film. The electrochemistry of the films in this region is not nearly as clean as in the electron-doping region as reflected in the sluggish response of the integrated charge curve and the fact that there is no peak for differential mobility at half charging, only a broad shoulder. From this shoulder, we can estimate the differential mobility for $1S_h$ holes to be approximately 0.6×10^{-3} $cm^2\ V^{-1}\ s^{-1}$. A more accurate value will have to await further improvements in the cross-linking of the nanocrystals. However, the hole mobilities appear to be of the same order of magnitude as the electrons. These preliminary results for hole conduction warrant further study and optimization of the cross-linking molecules for PbSe nanocrystals.

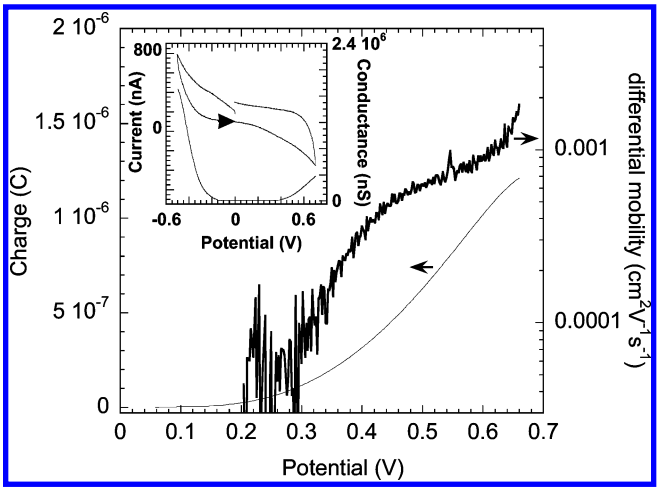

Figure 8. Differential mobility and integrated charge as holes are injected into a film of PbSe nanocrystals with a room-temperature first exciton at 0.66 eV. The data were taken at −49 °C with a scan rate of 10 mV/s while a 10.0 mV bias was applied between the working electrodes. The data are only shown for the anodic scan. Inset: cyclic voltammetry and conductance for the same scan as in the figure. The arrow shows the direction of the cyclic voltammetry. For clarity, the conductance data is shown only for the anodic direction.

C. Low-Temperature Conduction. To study the conduction of these nanocrystals further, the electrolyte was frozen while a thin film of PbSe quantum dots with a 0.7 eV first exciton was held in a charged state. Figure 9 shows several IV curves for this "frozen" film of PbSe quantum dots taken at different temperatures. Although the curves are quite linear at low bias for all temperatures, the inset shows that at higher bias the curves display a marked nonlinearity at low temperatures. All of the IV curves are symmetric around the zero point and displayed no hysteresis at scan rates used in the study.

Figure 10 shows the temperature dependence of the conductance of the film measured at a bias of 20 mV. The inset shows quite clearly that the conduction does not display Arrhenius-type temperature dependence and thus cannot be described as simply an activated process.

The non-Arrhenius behavior in this temperature range can be explained by a conduction model known as variable range hopping.[17] If we view the film of nanocrystals as a lattice of potential wells with a distribution of energies, then variable range hopping, proposed by Mott years ago to explain low-temperature conduction in amorphous semiconductors, states that the most probable electron hopping may not be between nearest-neighbor sites at low temperatures. This is due

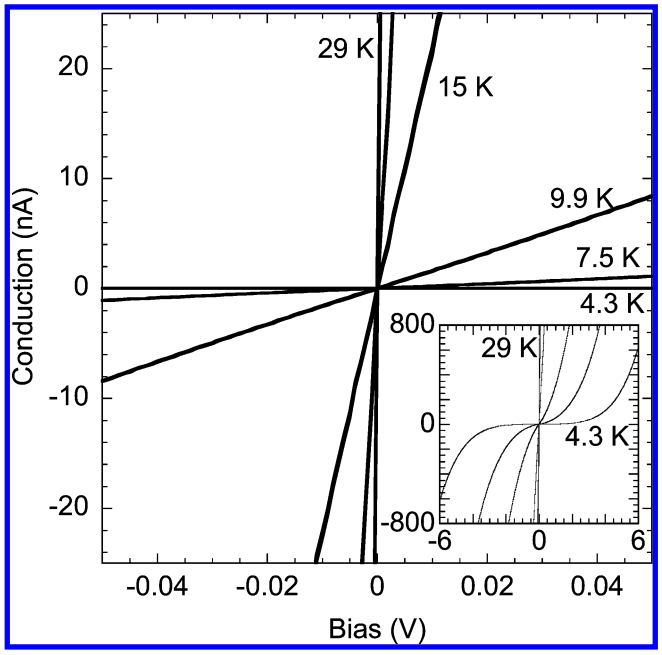

Figure 9. Low-bias IV curves of a film of PbSe nanocrystals on IMEs charged n-type and frozen. The nanocrystals have a 0.70 eV first exciton at room temperature. Inset: IV curves of the same sample taken with a larger bias range, displaying a nonlinear response.

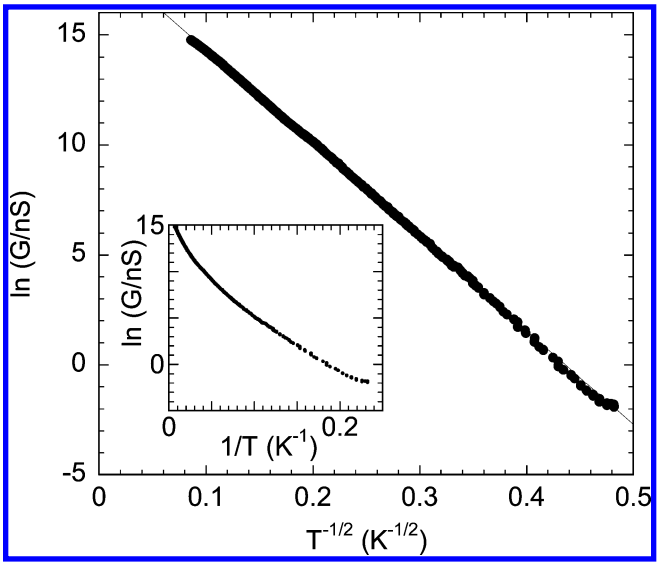

Figure 10. Temperature dependence of the low-bias (20 mV) conductance for a film of PbSe nanocrystals on IMEs. The film was charged n-type, and then the electrolyte was frozen. The data were taken in the 4.3−135 K temperature range. The nanocrystals have a 0.70 eV room-temperature first exciton. Inset: same data plotted to demonstrate the deviation from Arrhenius behavior in this temperature range.

to the fact that the energy cost to hop to a neighboring site may be larger than the cost to hop to a site that is further away. The probability, P, of an electron hopping from one site to another can be described by the equation

$$P \propto \exp\left(-\frac{2r}{a} - \frac{E}{k_B T}\right) \quad (1)$$

where r is the hopping distance, a is the localization length, and E is the activation energy.[17]

According to the variable range hopping model, the temperature dependence of the conductance, G, should follow the relation

$$G(T) \propto \exp(-(\beta/T)^{\nu}) \quad (2)$$

In Mott's original model, henceforth referred to as Mott's variable range hopping (M-VRH) model, $\nu = {}^1/_4$ for a 3D system. Later, Efros and Shklovskii expanded the model to include coulombic interactions between electrons.[18] This modification to Mott's model has the consequence of changing the temperature-dependent behavior of the conduction, so that at very low temperatures $\nu = {}^1/_2$. Henceforth, this modified model will be referred to as the Efros and Shklovskii variable range hopping (ES-VRH) model. As the temperature of the system increases, the coulombic interaction can be ignored and the system follows the $\nu = {}^1/_4$ law of M-VRH. The temperature at which the system goes from $\nu = {}^1/_2$ to $\nu = {}^1/_4$ behavior is T_C, which is given by the following relation

$$T_C = g\frac{e^4 a}{(4\pi\epsilon\epsilon_0)^2 k_B} \quad (3)$$

where g is the density of states at the Fermi level, and ϵ is the dielectric constant of the material. The value of T_C for materials such as amorphous semiconductors is usually very small, and thus, they follow the $\nu = {}^1/_4$ temperature dependence except at very low temperatures.

However, in films of colloidal semiconductor nanocrystals, the value of T_C should be much higher. Due to the fact that the electronic states of a single nanocrystal are discrete and atomic-like, an "artificial solid" fabricated from a fairly monodisperse sample of dots should have a relatively large density of states at energies corresponding to the electronic states of the individual nanocrystals. In a previous study of conduction in CdSe semiconductor nanocrystal solids, T_C was estimated to be ~400 K and the system was found to follow the $\nu = {}^1/_2$ law at temperatures below 160 K.[12] While the dielectric constant for bulk PbSe has a reported value of 280,[19] the dielectric constant for a film of PbSe nanocrystals has not yet been reported. This makes an estimation of T_C difficult at this point. However, since the temperature-dependent conductance data in Figure 10 fits the $\nu = {}^1/_2$ law quite convincingly, T_C must be greater than 135 K. Therefore, in this report, we will focus on the ES-VRH model.

In the ES-VRH model, β in eq 2 is replaced by the constant T^*, which is defined as[20]

$$T^* = \frac{2.8e^2}{4\pi\epsilon\epsilon_0 a k_B} \quad (4)$$

From a fit to the temperature-dependent conduction data shown in Figure 10, T^* has a value of 1800 K. This experimentally determined value of T^* is smaller than the experimentally determined value of $T^* = 5200$ K, found previously in the CdSe system.[12] This means that the conductance of a film of PbSe nanocrystals is less sensitive to temperature changes than a film of CdSe nanocrystals. By the use of the relation for T^*, a value for the dielectric constant of the film of PbSe can be estimated. The value for the localization length, a, is taken to be the radius of the nanocrystal, as it was in previous work on low-temperature conduction in CdSe films. From TEM measurements, the nanocrystals in this film were found to have a 6.3 nm diameter. Using eq 4 and the experimentally determined value of T^*, we can thus estimate ϵ to be ~8. While this value for the dielectric of the film of PbSe nanocrystals is larger than

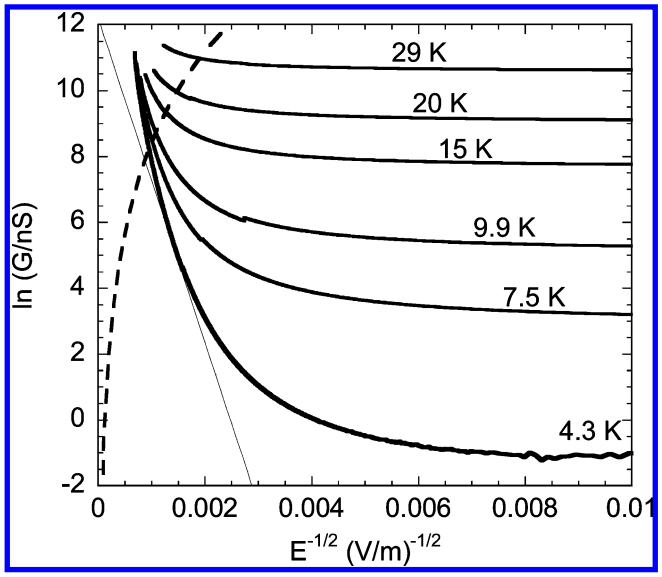

Figure 11. Field dependence of the conductance taken at several temperatures for a film of PbSe nanocrystals on IMEs which had been previously charged n-type and frozen. The dashed line shows the field and consequential conductance which delivers a thermal power of 1 mW to the sample. The thin line is the temperature-independent conductance curve described in the text.

that for a film of CdSe nanocrystal ($\epsilon = 4$),[14] it is quite small when compared to the dielectric constant of bulk PbSe.

With this estimated value of ϵ, we can return momentarily to the discussion of T_C. From a line width of ~90 mV for the first exciton, the volume of a nanocrystal, and the degeneracy of the $1S_e$ state, the density of states, g, can be estimated to be $\sim 2 \times 10^{45}$ J^{-1} m^{-3}. Plugging this value of g and the estimate of ϵ into eq 3, we find that T_C should be ~400 K, well above the temperature regime studied here. So, indeed, we are in the temperature region described by ES-VRH.

As shown in the inset of Figure 9, at high bias the IV curves become quite nonlinear. Figure 11 plots the field dependence of the conduction for several different temperatures in a different manner. Immediately, one notices that as the bias is increased the temperature dependency of the conduction is greatly reduced.

This field effect was noted in our previous study of the CdSe system and can also be accounted for by the ES-VRH model.[12] The external electric field serves to effectively reduce the barrier for hopping to downfield nanocrystals. In this model, large external fields lead to a temperature-independent conductance given by

$$G \propto \exp(-(E^*/E)^{(1/2)}) \tag{5}$$

where E^* is defined as

$$E^* = \frac{k_B T^*}{2ea} \tag{6}$$

This temperature independence can be understood from a simple qualitative argument. The field gives energy to the electron as it hops downfield, and this energy boost makes the site-to-site potential field appear smoother to the hopping electron, reducing the necessity at low temperature to look for more favorable sites toward which to jump.

Through the use of the experimentally determined value of T^*, the value of E^* for this system was calculated to be 2.4×10^7 V/m. A line representing this calculated temperature-independent conductance is shown in Figure 11. All the curves should asymptotically approach this curve at a high external field. It appears that the calculated value of E^* underestimates the true value by a fair amount. However, determining a value of E^* from the data is difficult because the curves only approach each other in the region where the dissipated thermal power becomes quite high. For reference, a line representing a thermal power of 1 mW across the film is drawn in Figure 11. In this high-power region, heating of the sample may also induce nonlinearities to the IV curves. Also, what makes the determination of E^* more difficult is the fact that the 4.3 K data does not follow a linear relation when plotted in this manner. This is in contrast to the CdSe data from our previous study, where the 4.3 K data is nearly linear when plotted in this fashion and all other temperature curves approach this temperature-independent conductance curve at much lower external fields.[12]

In addition to the value of T^* reported here, values three to four times smaller have also been seen in other films of PbSe nanocrystals. Perhaps this variability is due to a difference in film quality, the amount of capping molecules on the quantum dots, or the charging level at which the film was frozen.

As explained in the previous section, the electrochemistry of hole injection is not as clean or as complete as that for electron injection. This, coupled with an inevitable loss of charge during the freezing process, hampered the low-temperature study of hole-doped films. However, with a fair amount of difficulty, we have been able to freeze the holes into a PbSe thin film. The observed behavior of the hole-doped film is quite similar to that of the electron-doped film, as one would expect from the similar effective masses of the hole and electron in PbSe. The $\nu = 1/2$ law was observed in the 4.3−135 K range for hole-doped films, and a T^* of 1400 K was determined. The high-bias data obtained was qualitatively similar to the electron-doped material as well.

IV. Conclusion

Charge conduction in thin films of PbSe nanocrystals has been studied. By electrochemical gating, charges were injected into the quantum-confined states of the nanocrystals composing the films. Upon injection of charge into the films, a dramatic increase in conduction has been reported. As electrons are sequentially injected into the $1S_e$ and $1P_e$ states of the nanocrystals, the mobility of the electrons increased. A dip in the mobility of the $1S_e$ electrons was reported for half filling of the $1S_e$ state. Mobility as high as 5.0×10^{-3} cm^2 V^{-1} s^{-1} for electrons in the $1S_e$ state, corresponding to a conductivity of $\sim 2 \times 10^{-2}$ S cm^{-1}, was observed. The mobility of the holes in the $1S_h$ state of the nanocrystals was found to be an order of magnitude less than the mobility of electrons in the $1S_e$ state.

The behavior of charged films at temperatures between 4 and 135 K were explored by studying their IV curves. Low-bias conduction measurements revealed a temperature-dependent conductance of the form: $G(T) \propto \exp(-(T^*/T)^{1/2})$. At high bias, the IV curves displayed notable nonlinearities and the conductance approached a temperature-independent limit of the form $G \propto \exp(-(E^*/E)^{1/2})$. Further work on the molecular linkers in these films holds promise for even higher mobilities and more stable hole injection.

References and Notes

(1) Murray, C.; Sun, S.; Gaschler, W.; Doyle, H.; Betley, T.; Kagan, C. *IBM J. Res. Dev.* **2001**, *45*, 47.

(2) Wehrenberg, B.; Wang, C.; Guyot-Sionnest, P. *J. Phys. Chem. B* **2002**, *106*, 10634.

(3) Du, H.; Chen, C.; Krishnan, R.; Krauss, T.; Harbold, J.; Wise, F.; Thomas, M.; Silcox, J. *Nano Lett.* **2002**, *2*, 1321.

(4) Steckel, J.; Coe-Sullivan, S.; Bulovic, V.; Bawendi, M. *Adv. Mater*. **2003**, *15*, 1862.
(5) Schaller, R.; Petruska, M.; Klimov, V. *J. Phys. Chem. B* **2003**, *107*, 13765.
(6) Pietryga, J.; Schaller, R.; Werder, D.; Stewart, M.; Klimov, V.; Hollingsworth, J. *J. Am. Chem. Soc*. **2004**, *126*, 11752.
(7) Schaller, R.; Klimov, V. *Phys. Rev. B* **2004**, *92*, 186601.
(8) Ellingson, R.; Beard, M.; Johnson, J.; Yu, P.; Micic, O.; Nozik, A.; Shabaev, A.; Efros, A. *Nano Lett.* **2005**, *5*, 865.
(9) Qi, D.; Fischbein, M.; Drndic, M.; Selmic, S. *Appl. Phys. Lett.* **2005**, *86*, 93103.
(10) Morgan, N. Y.; Leatherdale, C. A.; Drndic, M.; Jarosz, M. V.; Kastner, M. A.; Bawendi, M. *Phys. Rev. B* **2002**, *66*, 75339.
(11) Yu, D.; Wang, C. J.; Guyot-Sionnest, P. *Science* **2003**, *300*, 1277.
(12) Yu, D.; Wang, C.; Wehrenberg, B.; Guyot-Sionnest, P. *Phys. Rev. Lett.* **2004**, *92*, 216802.
(13) Wehrenberg, B.; Guyot-Sionnest, P. *J. Am. Chem. Soc.* **2003**, *125*, 7806.
(14) Guyot-Sionnest, P.; Wang, C. *J. Phys. Chem. B* **2003**, *107*, 7355.
(15) Kang, I.; Wise, F. *J. Opt. Soc. Am. B* **1997**, *14*, 1632.
(16) Roest, A.; Kelly, J.; Vanmaekelbergh, D.; Meulenkamp, E. *Phys. Rev. Lett.* **2002**, *89*, 36801.
(17) Mott, N. F. *Conduction in Non-Crystalline Materials*; Clarendon Press: Oxford, U.K., 1993.
(18) Efros, A.; Shklovskii, B. *J. Phys. C* **1975**, *8*, L49.
(19) Boer, K. W. *Survey of Semiconductor Physics*; Van Nostrand Reinhold: New York, 1990.
(20) Shklovskii, B.; Efros, A. *Electronic Properties of Doped Semiconductors*; Springer-Verlag: Berlin, 1984.